Towards multifunctional building elements: thermal activation of a composite interior GFRP slab

Towards multifunctional building elements: thermal activation of a composite interior GFRP slab

D Khovalyg[1], A Mudry[1], M Pugin[1] and T Keller[2]

[1]Thermal Engineering for the Built Environment (TEBEL), Ecole Polytechnique Fédérale de Lausanne (EPFL), Switzerland
[2]Composite Construction Laboratory (CCLab), Ecole Polytechnique Fédérale de Lausanne (EPFL), Switzerland

E-mail: dolaana.khovalyg@epfl.ch

Abstract. Modular multifunctional building elements can overcome major disadvantages of the traditional sequential design and become prospective design solutions for sustainable construction. Thus, this work explores lightweight glass fiber-reinforced polymer (GFRP) profiles capabilities as multifunctional load-bearing slab modules in buildings. By adding water channels in a cellular structure of pultruded GFRP elements, hydronic radiant thermal conditioning of the indoor space can be enabled. Additionally, the water channels can protect critical slabs in case of a fire. A preliminary design of a multifunctional GFRP slab is performed for an office case study building by modifying a commercial slab profile with triangular channels. The thermal design load of the slab unit is determined using Rhino 6, and heat conduction and convective heat transfer for ceiling cooling and floor heating/cooling cases are investigated using ANSYS Fluent. The results show that a commercial GFRP profile can be modified to accommodate water channels and provide adequate heating and cooling at the upper or lower face. In addition, Serviceability Limit State is verified and required water flow adjustment in case of a fire outbreak scenario is discussed. Thus, the GFRP radiant slab has the potential as a pre-fabricated alternative for traditional embedded radiant systems.

1. Introduction

Traditional sequential design of building envelope where every element performs only one dedicated function is obsolete, carries significant embodied energy, complicates quality control, requires a vast amount of coordination at the building site, and prolonged construction time. The alternative and innovative solutions are modular pre-fabricated multifunctional building elements that can overcome the major disadvantages of the current practice and go beyond. Although concrete and steel are the most widely used structural materials, glass fiber-reinforced polymers (GFRP) are perspective structural materials [1]. GFRP is made from glass fibers and a polymer matrix aggregating the fibers, and the advantages of this material compared to concrete and steel are its lightweight, high specific stiffness and strength, durability, chemical resistance, and low thermal conductivity. The structural and durability properties are the main reasons why GFRP is gaining use in construction. In contrast to bridge construction, building structures are most of all still prototypes, like the Futuro House made by Matti Suuronen in the 1960s, and the Eyecatcher Building located in Basel, Switzerland, from 1999 [2]. Low fire resistance of GFRP structures has hindered widespread application in building construction so far.

GFRP elements are usually pultruded in constant cellular cross-sections or conceived as sandwich structures with complex core assemblies manufactured through vacuum-assisted resin infusion. Such

cellular structures can be advantageous if they can be filled in with appropriate media to elevate the functionality of the GFRP element. If necessary, customized cells can also be developed. By adding water channels in the core of the slab, not only active heating/cooling can be embedded into the lightweight structural element, but also fire protection can be added. Addressing fire resistance by adding water cavities has been investigated at CCLab at EPFL and resulted in the successful development of GFRP elements for multi-story buildings [3]. The feasibility of the multifunctional GFRP slab with an embedded radiant system for a selected commercial building is studied in this work from a structural and thermal perspective.

2. Methodology

Since no prior studies on using the GFRP modules as thermally activated building elements are available, the multifunctional GFRP module structure is built up from the existing commercial bridge decking Asset-type system FBD600 produced by *Fiberline,* having triangular cells where inclined webs carry the shear forces (Figure 1a). To circulate water flow closer to the flanges, water channels are created inside the cells, as shown in Figure 1(b). Water-filled channels facing the upward face can provide active heating of the indoor space above the slab, while water circulating inside the bottom channels can provide cooling for the space below the slab. In addition, the flow of water in the cavities can help to resolve the main drawback of GFRPs in building applications – low fire resistance. To meet the required thermal resistance of the building element, the remaining cavities can also be filled with polyurethane foam.

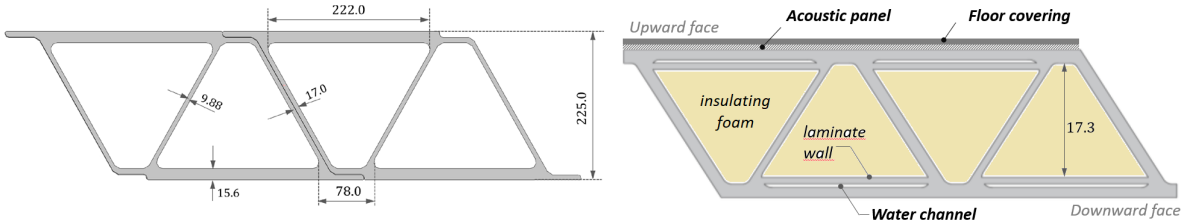

Figure 1. Cross sections of GFRP Asset-type profiles (dimensions are shown in mm): (a) original profile, (b) modified profile to accommodate water channels.

While GFRP laminate walls separating the water channel from the main cell can be 5 mm (the minimum possible thickness), the height of the water channels is unknown at the beginning. Since each channel is relatively wide (222 mm), the height of channels is estimated to be quite small if a proportional volume of water for a regular embedded radiant system is considered. By considering regular embedded floor radiant systems with piping of 12.7-25.4 mm and spacing between the pipes of 150-300 mm [4], the height of the channels is initially considered as 5 mm. The final height needs to be determined by knowing how much water should be circulated to provide the required heating and cooling for the maximum demand and fire resistance of the structure. Therefore, the definition of channel geometry and performance of the multifunctional GFRP element is an iterative process.

To analyze structural performance and design thermal loads, as a case study building, an existing 5-story office building located at the Innovation Park – EPFL in Lausanne (46.5166 N, 6.56265 E) is chosen. The interior dimensions are 29.3 m x 29.3 m, and the footprint area is 859 m^2; the ceiling height is 3.51 m. The glazing covers 50% of the façade area. The core of the building is reserved for the stairs and bathrooms and an atrium that connects each floor with the rest of the building. To simplify the thermal analysis, the atrium is not considered. Moreover, the office space is simplified to a large open space without interior walls. Only the 3^d floor of the building is analyzed since its ceiling and floor are indoor slabs. The open space is divided into 14 square zones of 7.2 x 7.2 m^2 according to the load-bearing structure, as shown in Figure 2.

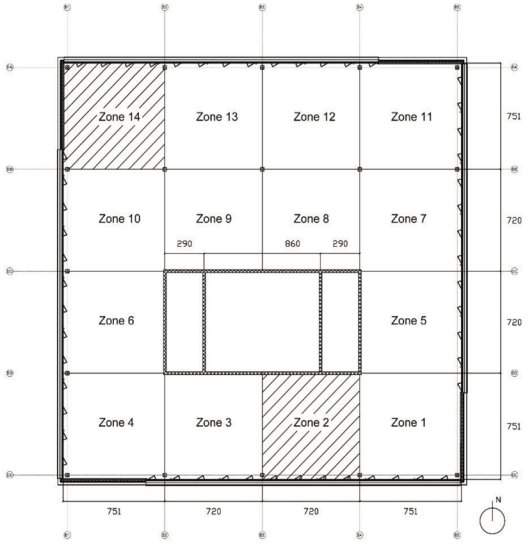

Figure 2. Floor plan of the case study building.

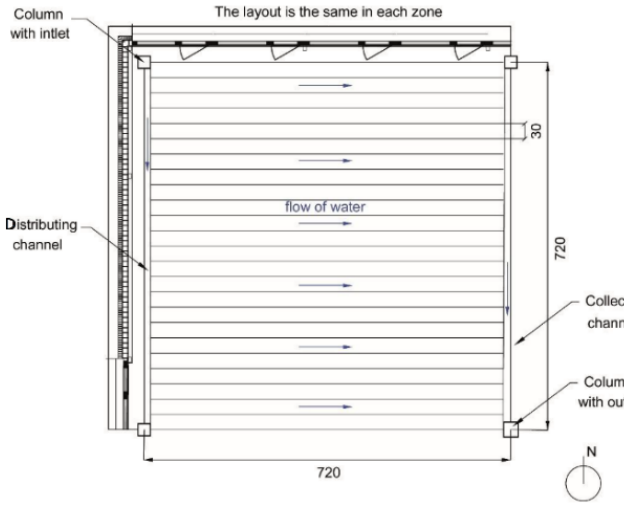

Figure 3. Water distribution (shown for one zone).

2.1. Structural performance

The permanent loads g_k are determined for the slab materials: 1.04 kN/m for GFRP, 0.04 kN/m for the floor covering, 0.17 kN/m for an acoustic panel, 0.10 kN/m for water, and 0.07 kN/m for an insulation foam. Since the case study building is an office building, Cat. B live loads q_{k1} are considered as 3 kN/m^2 according to the Swiss national standard SIA 261. For the Serviceability Limit State verification, the frequent and almost permanent loads q_d are determined according to SIA 260. The reduction coefficients $\psi_{11} = 0.5$ for frequent loads and $\psi_{21} = 0.3$ for almost permanent loads are selected from SIA 260. Creep deformations are neglected, as suggested by the manufacturer of the GFRP profiles.

To verify the structural performance of the GFRP slab, it is critical to verify the Serviceability Limit State (SLS). The Ultimate Limit State (ULS) is normally not critical considering the high strength of the GFRP profile ($f_{t,x}$=350 N/mm^2, $f_{c,x}$ =205 N/mm^2, $f_{f,x}$=300 N/mm^2 per [5]). The slab elements must be supported by longitudinal supports (walls or beams). For the case study building, the slab elements are supported by beams (which are supported by columns). The SLS needs to be verified for 3 different cases "*operations-frequent loads*", "*comfort-frequent loads*", and "*aspect-almost permanent loads*" by calculating the deflection $w = (5/384) \cdot (q_k \cdot L^4/E \cdot I)$ of the slab and comparing it with limiting value w_{max} outlined by SIA 260. The moment of inertia of the slab I is determined with the Steiner Rule; Young modulus E of the Asset FBD 600 profile is 20 MPa. The contribution of the web to the moment of inertia has been neglected. The maximum span of the slab is $L_{max} = \sqrt[3]{(384 \cdot E \cdot I)/(5 \cdot F \cdot q_k)}$ (where F=350 for operations/comfort – frequent loads, and F=300 for aspect-almost permanent loads).

2.2. Definition of the thermal design loads

2.2.1. Thermal demand of a case study building. The building thermal loads are simulated using a building energy simulation tool Rhino 6 with plugins Honeybee and Ladybug. The input parameters for energy simulations such as building envelope properties, internal loads, schedules are defined according to SIA 380/1, SIA 2024, and SIA 2028. Multiple scenarios have been analyzed, including concrete and timber walls. U-values of exterior and interior walls are taken as 0.285 W/m^{2}K and 0.288 W/m^{2}K for the concrete wall case, and as 0.244 W/m^{2}K and 1.61 W/m^{2}K for the timber structure case. U-value of windows is considered as 1 W/m^{2}K, and two solar heat gain coefficients (0.7 and 0.55) are explored. Scenarios with no operating shades and with operating shades drawn down at 200 W/m^2 are considered. Indoor operative temperature (*Top*) settings are determined according to Cat. II of thermal comfort outlined in ISO 17772-1:2017. For the minimum load scenario, the heating setpoint (H) and the cooling

setpoint (C) should be 20°C and 26°C, respectively, which would result in a minimum operation of the HVAC system. For the maximum load scenario, the heating setpoint is taken as 22.5°C, and the cooling setpoint is 23.5°C. Temperature setpoint is considered as constant over 24 hours. An overview of different scenarios to define the thermal loads is shown in Table 1.

Table 1. Overview of different scenarios for building energy simulation.

Scenario	*Concrete walls*	*Timber walls*	*Solar factor g=0.7*	*Solar factor g=0.55*	*T_{op} (H) 20°C*	*T_{op} (H) 22.5°C*	*T_{op} (C) 26°C*	*T_{op} (C) 23.5°C*	*Shades OFF*	*Shades ON at 200 W/m²*
1	x		x		x		x		x	
2	x		x			x		x	x	
3		x	x			x		x	x	
4	x			x		x		x	x	
5	x		x			x		x		x

2.2.2. Definition of the thermally active surface area. Once the thermal demand of the case study building is determined, the active surface area needs to be calculated by defining the layout of the water flow. Typically, the layout of the radiant hydronic piping is serpentine and counter-flow. Since turning bends are difficult to implement in the GFRP slab structure, a parallel flow of water in the channels is considered (Figure 3). Water in one zone can be distributed from a large channel at one side of the zone and collected at the other side of the zone. In order to reduce the channel length, head loss, and the complexity of the water distribution network, water should be distributed and collected for each individual zone through the nearby columns located in two opposite corners in diagonal of the zone, permitting a relatively equal flow rate and pressure loss between the parallel channels. Therefore, it is considered that the columns are hollow-core square columns. For example, for zone 14 shown in Figure 3, the column in the peripheral area (close to the exterior wall) is distributing water, allowing the circulation of the warmest water in the zone close to the exterior boundary (the one with the major heat losses/gains) and the column at the opposite (in diagonal) is collecting the water.

2.2.3. Definition of the limiting heat fluxes from the surfaces. To assure the comfort of occupants, not only the indoor operative temperature range but also surface temperatures should be limited. ISO 7730:2005 specifies limits of surfaces as 29°C for floor heating and 17°C for ceiling cooling. In addition, for cooling scenarios, the surface temperature should be higher than the dew point temperature of the room to avoid any condensation. Thus, the dew point temperature limit is considered as 16°C at the design stage. Based on ISO 11855-2:2012, the limiting heat fluxes for floor heating and ceiling cooling can be estimated using specific equations such as $q = 8.92 \cdot (\theta_{sm} - \theta_i)^{1.1}$ for floor heating and ceiling cooling, and $q = 7 \cdot (\theta_{sm} - \theta_i)$ for floor cooling. In each case, the difference in surface temperature θ_{sm} and indoor operative temperature θ_i, and overall heat transfer coefficient are considered. The limiting heat fluxes are compared with the case study thermal loads, and thermal design loads are identified to proceed further with water flow analysis.

2.3. Hydronic system analysis

2.3.1. Conduction heat flow through the slab. Average water temperature is determined by solving conduction heat transfer from the surface to the water channels. Standards ISO 11855-2:2012 and ISO 11855-3:2012 provide a methodology to calculate the average water temperature for conventional radiant systems by using characteristic curves. However, there is no explicit methodology on how to proceed with customized systems. Therefore, the thermal resistance method is used to determine linear heat flow through conductive layers. Thermal resistance through the part of the GFRP slab with a water channel is defined as $R = 1/h_i + \sum(s_i/\lambda_i)$, where h_i is total heat transfer coefficient (11W/m²K for floor heating and ceiling cooling, and 7 W/m²K for floor cooling). The thickness of each layer s_i and conductivity λ_i are provided in Table 2, in addition to density ρ and specific heat C_p. The acoustic panel is placed underneath the floor covering.

Table 2. Properties of the materials of the slab.

Layers	*s (mm)*	*λ (W/mK)*	*ρ (kg/m³)*	C_p *(J/kgK)*
Floor covering (linoleum)	2.5	0.1900	1200	1400
GFRP layers	15.6 x 2, 10	0.3500	1870	1170
Polyurethane foam	188.8	0.0325	45	1500
Acoustic panel	15.0	0.3200	1150	1100

2.3.2 Water flow analysis. Analysis of the hydronic system consists of determining the water flow rate and the head loss, enabling optimal cross-section. The mass flow rate of water for a particular thermal load of the zone is determined per ISO 11855-3:2012 equation $m = (q \cdot A_F)/(C_p \cdot \sigma) \cdot [1 + R_i/R_u + (\theta_i - \theta_u)/(q \cdot R_u)]$, where q is the thermal load, A_F the thermally active surface area, σ the temperature drop between water inlet and outlet (considered as 3 K), R_i and R_u are the thermal resistances of the structure above (i) and under (u) the water channel, and θ_i and θ_u are the indoor operative temperatures of the space above and under the slab. Water velocity is defined by knowing the mass flow rate, water density, and cross-section of the channel. Important to mention is that maximum water velocity is limited to 1.2 m/s per ISO 11855-1:2012 to minimize possible noise from the water flow, while pressure drop is limited to 400 Pa/m. Linear head loss ΔP is determined from the Darcy-Weisbach equation by considering the friction factor for smooth surfaces, and hydraulic diameter of $2 \cdot h$ for parallel plate flow since the width of the water channel is much longer than its height. Maximum water velocity and head loss determine the optimal height of the water channel (the length of the channel is already defined by the considered geometry of the slab). Procedures described in Section 2.2 need to be repeated if the initially assumed height of the water channel does not provide acceptable water velocity (1.2 m/s) and head loss (400 Pa/m).

2.4. Thermal performance analysis

Once the design thermal loads are determined and the geometry of the channel is finalized, the GFRP structure is modeled in ANSYS software from ANSYS Inc. Detailed heat transfers analysis and water pressure losses are obtained using CFD analysis. Particularly, temperature variation along the surface of the slab and across the slab is analyzed. To compare the performance of the selected GFRP profile, a conventional radiant system is modeled in HEAT2, and the temperature distribution at the surface of the slab is compared with the GFRP radiant system.

2.5. Fire protection

The bottom flange, at the ceiling level, is the structural part of the slab that needs to be protected at most. In case of a fire outbreak, the temperature there would be much higher than at the floor level. The flange is protected when the temperature of its interior surface, at the water side, is kept below 50°C [3]. In such as case, the resin of the GFRP layer with the minimum thickness does not reach the glass transition temperature, and the layer remains able to carry the load. Since the heat output of the fire is much higher than the design thermal load of the radiant systems, the water flow rate must be increased, and water temperature should be decreased. In such a case, the main objective is to analyze the magnitude of water velocity and head loss at the increased flow rate required to withstand the fire heat input. As heat input to the water channel, the testing results from [3] are used. Although a different kind of GFRP profile (DuraSpan) was tested, by considering the total area exposed to fire, the heat input for the Asset-type profile can be determined. It is twice as much as from the test in [3], and about 15.9 kW per water channel.

3. Results

3.1. Structural performance

The SLS verification is determined for a 1 m width of the cross-section shown in Figure 2(a). Once the moment of inertia of the slab is calculated ($I = 3.34 \cdot 10^8$ mm^4), the actual deflection for the 3 cases

defined above is determined and compared with the limiting values. As shown in Table 3, the deflection $\boldsymbol{w}$ is lower than the maximum value w_{max}; thus, the SLS is verified. The maximum span of the slab is 8 m; therefore, the span of the case study building of 7.2 m is permitted.

Table 3. Serviceability Limit State verification.

Type of verification	w (mm)	w_{max} (mm)	L_{max} (m)	Verification
Operations – frequent loads	14.9	20.6	8	√
Comfort – frequent loads	7.7	20.6	10	√
Aspect – almost permanent loads	11.8	24.0	9.1	√

3.2. Design thermal demand and water flow parameters

Building energy simulation results show that in all 5 cases listed in Table 1, zone 14 in the NW corner has the maximum heating load between 31-36 W/m^2. In 4 out of 5 scenarios, zone 2 in the South has the highest cooling load of 73-92 W/m^2. Only in scenario 5, the cooling load is 42 W/m^2 in zone 4. The maximum heating demand of 36 W/m^2 occurs in scenario 5 in zone 14 due to the low *g*-value of windows and high heating operative temperature setpoint. The maximum design cooling load of 92 W/m^2 occurs in zone 2 of scenario 3. It is due to the low *g*-factor of windows, no solar protection on windows, and, finally, timber structure of walls. The timber structure has lower thermal inertia than concrete walls; thus, it has a reduced capacity to store thermal energy and shift the peak cooling load. For further analysis, maximum thermal loads are considered normalized by the active surface area, resulting in 39 W/m^2 of heating and 96 W/m^2 of cooling design heat fluxes.

Based on the methodology described in Section 2.2.3, the limiting surface heat flux to avoid local discomfort due to low or high surface temperature is determined. It is 100 W/m^2 and 70 W/m^2 for floor heating at operative temperatures of 20°C and 22.5°C, respectively. Similarly, it is 100 W/m^2 and 70 W/m^2 for ceiling cooling at operative temperatures of 26°C and 23.5°C, respectively. The limiting heat fluxes for heating are much higher than the design heat flux, while the design heat flux for cooling reaches the limiting values. High cooling load, considered based on scenario 3, can be reduced by increasing the operative temperature, as in scenario 1, or by implementing shades, as it is in scenario 5. In such a case, the cooling heat flux can be reduced down to 86 W/m^2 and 45 W/m^2, respectively. Since, in practice, little is known regarding the operative parameters of the new building at the design stage, it is better to design a GFRP system that can be universal and cope with the highest cooling load of 96 W/m^2 determined from scenario 3. In such a case, cooling can be provided jointly by the floor and by the ceiling. The floor cooling system can absorb up to 49 W/m^2 at 26°C and 32 W/m^2 at 23.5°C by accounting for the limiting floor surface temperature of 19°C.

A summary of selected design cases for floor heating (FH), ceiling cooling (CC), and floor cooling (FC) are listed in Table 4. In the same table, the calculated water flow parameters are provided. Water flow is always laminar, and pressure drop is relatively low (less than 14.4 Pa/m). The corresponding maximum head loss is 0.25 m.

Table 4. Flow parameters for each design case.

Scenarios	Case abbreviation	Design heat flux (W/m^2)	Operative temperature (°C)	Actual heat flux (W/m^2)	$\Delta q_{dsn-act}$ (%)	Mean water temperature (°C)	Flow velocity (cm/s)	Reynolds Number (-)	ΔP (Pa/m)
Floor Heating	FH 20-100	100	20.0	91.3	8.7	39.0	1.60	222	10.8
	FH 22.5-70	70	22.5	63.5	9.3	35.8	1.13	156	7.4
	FH 22.5-39	39	22.5	35.2	9.6	29.9	0.62	86	5.4
Ceiling Cooling	CC 26-100	100	26.0	90.0	9.8	12.5	1.59	121	14.4
	CC 23.5-70	70	23.5	64.1	8.5	13.7	1.11	85	11.3
	CC 23.5-45	45	23.5	40.8	9.4	17.2	0.72	55	10.6
Floor Cooling	FC 26-49	49	26.0	45.6	7.0	13.7	0.79	61	6.1
	FC 23.5-32	32	23.5	29.8	7.0	15.5	0.51	39	4.2

3.3. Surface and 2D temperature distribution

For the thermal performance analysis, a section of the slab is analyzed rather than a full slab of 7.2 m x 7.2 m. The analyzed portion of the slab has a width of 1.2 m at the upper face (floor level) and 1 m at the lower face (ceiling level); the length in the longitudinal direction is 1 m. The slab section has 5 cells in total; 3 water channels are for floor heating/cooling, and 2 channels are for ceiling cooling. The temperature distribution for cases listed in Table 4 is shown in Figure 4. Generally, the surface temperature is very uniform above the channels, while there is a temperature drop between the channels due to the low heat conduction between the adjacent channels. The magnitude of the temperature variation above the channels and in-between the channels is the greatest for high heat flux cases such as FH 20-100 (4.8 K), CC 26-100 (2.5 K), and FC 26-49 (2 K). It is the lowest for the low heat flux cases such as FH 22.5-39 (1.7 K), CC 23.5-45 (1.4 K), and FC 23.5-32 (1.2 K). In all cases, the maximum surface temperature does not exceed the limiting temperature (29°C for floor heating, 19°C for floor cooling, and 17°C for floor cooling). Simulations show that the actual heat flux is slightly lower than the design heat flux, and the difference $\Delta q_{dsn-act}$, as listed in Table 4, is between 7-9.8%.

To understand the difference in the thermal performance of the GFRP radiant system compared to conventional radiant systems, the case of floor heating FH 20-100 is compared with a radiant embedded heating system set for the same design heat flux according to the example in Annex D of ISO 11855-2:2012. Two cases of spacing are compared, 150 mm and 300 mm. Conventional embedded systems with round piping exhibit a sinusoidal temperature variation at the surface. In the case of the piping with 150 mm spacing, the period of fluctuations is 0.2 m, and the amplitude of temperature variation is 1.5 K (27.5-29°C). In the case of the piping with 300 mm spacing, the period of fluctuations is 0.4 m, and the amplitude of temperature variation is 4.5 K (24.3-29°C). Therefore, the GFRP system can provide a much more uniform surface temperature than the conventional embedded system, even though there is a pronounced temperature dip in-between the channels.

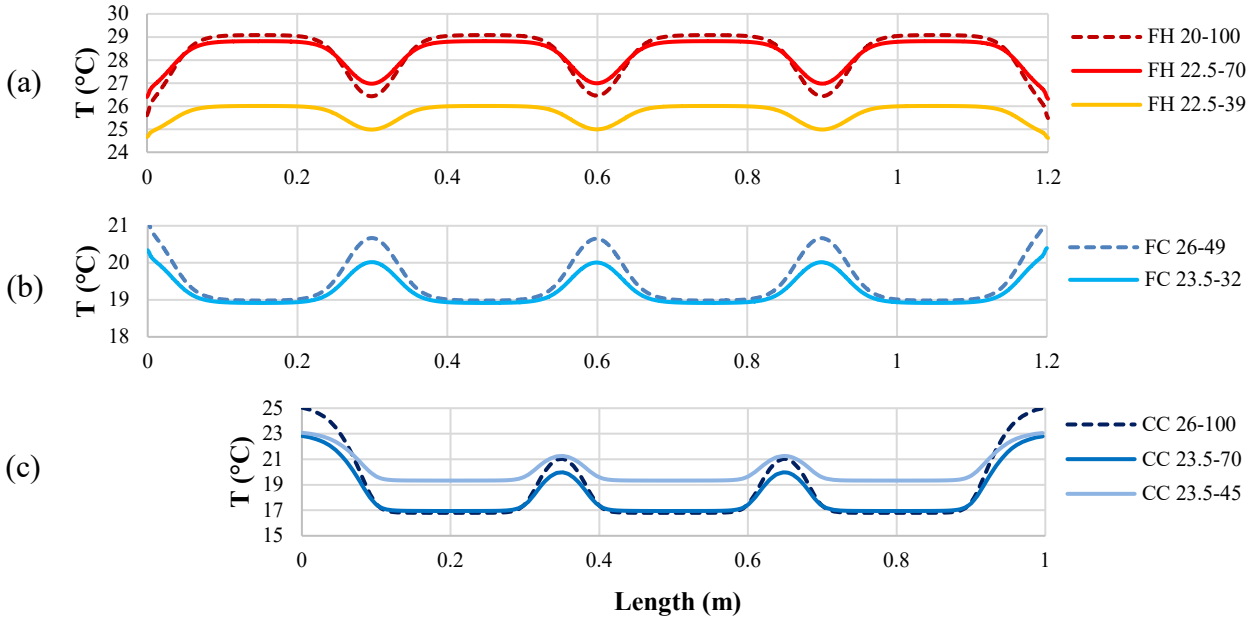

Figure 4. Surface temperature distribution: (a) floor heating, (b) floor cooling, (c) ceiling cooling. "Tails" at the beginning and the end are due to the edges of the profile.

In addition to the surface temperature analysis, the 2D temperature distributions across the cross-section of the GFRP profile are investigated. Three fragments of the GFRP cells for the highest heating/cooling cases are shown in Figure 5. According to Figure 5(a), there is almost no heat transfer between the upper and lower face of the slab (between the rooms above and below the slab). Insulation in the cells and low conductive GFRP webs prevent downward heat loss from the channel with warm

water on top. The temperature variation in the slab is quite linear. The upper layer of the floor acts as an insulator and decreases upward heat conduction. The overall temperature distribution behavior is similar for the cooling cases shown in Figures 5(b) and 5(c). There is limited heat conduction between the upper and lower face of the slab; the coldest area is primarily around the channels with cold water. A non-conditioned face has a uniform temperature, and there are limited conduction in-between channels. Since initially considered cross-section of the channels with a height of 5 mm provide adequate thermal performance, their size is not modified further and considered for the following fire protection analysis.

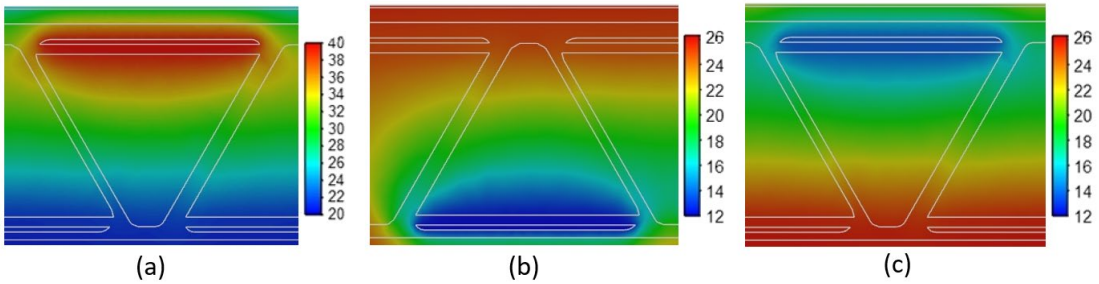

Figure 5. Cross-sectional temperature distribution: (a) FH 20-100, (b) CC 26-100, (c) FC 26-49.

3.4. Fire protection

To analyze the fire outbreak scenario, the water supply temperature is taken as 25°C (appx. at room temperature), and the temperature difference between inlet and outlet is kept below 25 K to make sure that water along the entire length of the profile stays under 50°C. To remove 15.9 kW of heat per channel surface area of 1.6 m^2 (only area exposed to the fire), the water flow rate needs to be significantly increased. The volumetric flow rate per channel should be 0.55 m^3/h resulting in a water velocity of 13.7 cm/s. The resulting pressure loss is 82 Pa/m, and the total head loss is 1.45 m. This value is nearly 6 times higher than the maximum head loss of the GFRP radiant systems analyzed, meaning that a more powerful pumping system needs to be activated in case of a fire outbreak.

4. Conclusions

This work presents a feasibility study for a multifunctional GFRP slab including structural and thermal performance considerations. Since a GFRP radiant system is a novel system, there is no design methodology developed yet; this work illustrates the preliminary design flow for a specific office case building and its thermal loads. First of all, structural performance is verified before proceeding to the thermal analysis. Secondly, thermal design loads for each thermal zone of a case study building are determined. By assuming the height of the water channels, thermal and hydraulic analysis is performed. In this particular case, the initial geometry of the channels is suitable, and no iteration is performed. Lastly, the possibility of the water flow to remove the heat input in case of a fire outbreak is shown. Further analysis requires validation of the acoustic performance, design of the inlet and outlet water manifolds and connections, and a life cycle assessment of the system to evaluate its environmental impact. Also, the dynamic thermal behavior of the GFRP radiant slab needs to be simulated. Moreover, the GFRP profile can be customized for this specific application in buildings, and its thermal and structural performance can be elevated by locally adding carbon fibers. Even though there are many open questions remaining, this work illustrates that a thermally activated GFRP slab can be a promising solution to shift towards the multifunctional and pre-fabricated structural elements in buildings.

References

[1] Bai J 2013 *Advanced fiber-reinforced polymer (FRP) composites for structural applications.* (Woodhead Publishing)
[2] Keller T, Theodorou N, Vassilopoulos A and de Castro J. 2016 *J Compos Constr* 20(1) 04015025
[3] Keller T, Tracy C and Hugi E 2006 *Composites Part A* 37(7), 1055-67
[4] Uponor 2011 *Uponor - Complete Design Assistance Manual* p.380
[5] Fiberline Composites 2017 *Values for global analysis, FBD 300*